ChemComm

COMMUNICATION

View Article Online
View Journal | View Issue

Fluorescent detection of RDX within DHPA-containing metal–organic polyhedra†

Cite this: *Chem. Commun.*, 2014, **50**, 3467

Received 10th December 2013,
Accepted 21st January 2014

DOI: 10.1039/c3cc49355e

www.rsc.org/chemcomm

Liang Zhao, Yulu Chu, Cheng He and Chunying Duan*

By incorporating the dihydropyridine amido (DHPA) group into the rationally designed ligand systems, metal–organic molecular polyhedra were obtained *via* self-assembly for the luminescent sensing of highly explosive RDX with a limit of detection lower than 1 ppb in solution.

Detection of hidden explosive devices in minefield remediation,[1] crime scene investigations[2] and counter-terrorism applications such as personnel or baggage screening, facility protection, and cargo screening[3] is a pressing concern. The need for ultratrace detection of the commonly used powerful explosives having low-volatility has resulted in an intense interest in fluorescence methods. And numerous optical[4,5] and electrochemical sensors[6,7] for nitroaromatic compounds were developed recently. While cyclotrimethylene trinitramine (RDX) is more powerful than TNT, few high sensitivity RDX probes that exhibit satisfactory properties have been reported, due to the fact that RDX is nonaromatic, it exhibits a three-dimensional flexible structure and just contains one kind of recognition unit (nitramine). By modifying the reduced nicotinamide adenine dinucleotide (NADH) analogue as a reducing agent, metal–organic complexes[8] and CdSe–ZnS QDs[9] have been created for the fluorescent detection of RDX. It is thus hypothesized that the development of three dimensional capsules with appropriate sizes and NADH analogues as suitable triggers represents a powerful strategy to create RDX sensors with high selectivity and sensitivity.

Metal–organic polyhedra, discrete molecular architectures that are constructed through the coordination of metal ions and organic linkers, have attracted considerable attention due to their potential for a variety of applications due to their high symmetry, stability and rich chemical/physical properties.[10–14] The architectures that generate well-defined cavities with gated pores provide specific inner environments for the selective uptake and bonding of guest molecules and the catalysis of their reactions.[15] By incorporating N_2O chelators within the ligand backbone, a series of metal–organic polyhedra and cyclohelicates have been constructed and used as efficient chemosensors for the selective and sensitive detection of guest molecules with different sizes, shapes and interaction handles. As the dihydropyridine amido (DHPA) group is described as the key structure in NADH models[16] and plays an important part in the electron transfer process, herein, we report the assembly of Ce–**ZPS** and Zn–**ZPT** (see Scheme S1 in the ESI†) metal–organic polyhedra through combination of the DHPA group with the rationally designed ligand systems. We envisioned that these capsules would be promising chemosensors for RDX. The well-positioned DHPA would provide appropriate matches for polar groups to address the structural diversity of RDX and that the difficulty of selectively recognizing flexible conformations of RDX could be overcome. And these oxidized DHPA fragments possibly exhibited obvious emissions to transform this selective recognition information into measurable luminescent signals. Experimental results suggested that the metal–organic octahedron Zn–**ZPT** can function as an enzyme-like pocket to encapsulate the explosive RDX molecule and prompt the photoreaction with the **DHPA** group with a *ca.* 27 fold luminescent enhancement and the limit of detection was improved to 1 ppb.

Ligand H_6**ZPS** was synthesized from salicylaldehyde with 1-(4-(hydrazinecarbonyl)phenyl)-4-phenyl-1,4-dihydropyridine-5-dicarbohydrazide in an ethanol solution and characterized by elemental analysis and spectroscopic methods. Evaporating a DMF solution of H_6**ZPS** containing $Ce(NO_3)_3{\cdot}6H_2O$ generated Ce–**ZPS** in a high yield (57%). Single-crystal X-ray structural analysis confirmed the formation of a $Ce_4(H_2$**ZPS**$)_4$ tetrahedron with a crystallographic C_3 symmetry in the solid state (Fig. 1).[17] The tetrahedron comprised four vertical metal centers and four deprotonated H_2**ZPS** ligands. Each cerium ion was chelated by three tridentate chelating groups from three different ligands to form a ternate coronary trigonal prism coordination geometry. The four pseudo-C_3 symmetric ligands positioned individually on the four triangle faces of the tetrahedron were defined by four metal ions. The Ce···Ce separation was ~13.57 Å, the inner volume of the tetrahedron was about 350 Å^3. The rhombic window of the tetrahedron had a size of 6.8 × 6.5 Å^2, potentially allowing the ingress and egress of small molecules *i.e.* RDX.

State Key Laboratory of Fine Chemicals, Dalian University of Technology Dalian, 116012, China. E-mail: cyduan@dlut.edu.cn

† Electronic supplementary information (ESI) available: Experimental details and additional spectroscopic data. CCDC 972499. For ESI and crystallographic data in CIF or other electronic format see DOI: 10.1039/c3cc49355e

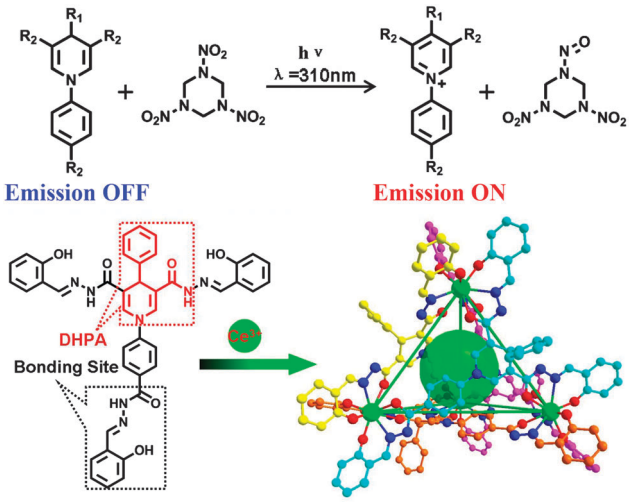

Fig. 1 The constitute/constructional fragments of Ce–**ZPS**. H atoms and solvent molecules are omitted for clarity. The metal, oxygen and nitrogen atoms are drawn in green, red and blue respectively. The carbon atoms are drawn in other colours. Selected bond distances (Å): Ce–O_{phenol} 2.20, Ce–$O_{carbonyl}$ 2.44, Ce–N 2.65.

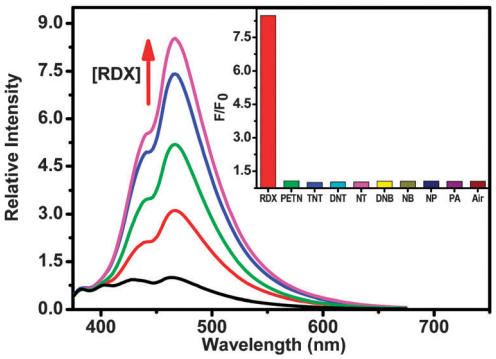

Fig. 2 The time-dependent fluorescence growth of Ce–**ZPS** (10 μM) in a DMF solution upon addition of RDX (1 μM) after irradiation with 310 nm light. Spectra were recorded at time intervals of 1 min. The inset shows the fluorescence responses of Ce–**ZPS** towards RDX over various explosives with the emission intensity at 465 nm after a 5 min irradiation (excitation at 350 nm).

The benzene ring of DHPA was positioned outside of the tetrahedron and its active site positioned in the interior of the cavity. These DHPA moieties thus provided geometric, coordinative and functional properties to the cage-like capsule, ensuring the size and shape selectivity for this host–guest complexation behaviour. The C–N (DHPA) distance of 1.39 Å is a formal single bond, indicating the reduction state of the ligand. The C–O and C–N distances of 1.26 Å and 1.32 Å, respectively, within the ligands were intermediate between formal single and double bonds, indicating the extensive delocalization over the entire molecular skeleton.[18] Such a conjugated system is beneficial to the signal transduction within the ligand backbone and it potentially enhances the fluorescence response upon interaction with guests.

ESI-MS spectra of Ce–**ZPS** in a DMF–CH_3CN solution exhibited intense peaks at m/z = 1710.24, 1741.73 and 1773.23 with the isotopic distribution patterns separated by 0.50 Da, assignable to $[Ce_4(H_2\mathbf{ZPS})_2(H\mathbf{ZPS})_2]^{2-}$, $[Ce_4(H_2\mathbf{ZPS})_2(H\mathbf{ZPS})_2{\cdot}2CH_3OH]^{2-}$ and $[Ce_4(H_2\mathbf{ZPS})_2(H\mathbf{ZPS})_2{\cdot}4CH_3OH]^{2-}$, respectively, indicating the successful assembly of a Ce-based M_4L_4 tetrahedron. Upon the addition of RDX, ESI-MS spectra exhibited a new peak at m/z = 1821.26. An exact comparison of this peak with the simulation results obtained on the basis of natural isotopic abundances revealed the assignment of the peak to the species $[Ce_4(H_2\mathbf{ZPS})_2(H\mathbf{ZPS})_2 \supset RDX]^{2-}$, demonstrating a 1:1 stoichiometric inclusion behavior. These results suggested that the cavity of the Ce–**ZPS** tetrahedron could encapsulate RDX directly, in which the encapsulated RDX reacted with DHPA efficiently to form highly luminescent active species for the experimental detection.

Compound Ce–**ZPS** (10 μM) exhibited an absorption band centered at about 390 nm in DMF solvent ($\log \varepsilon$ = 5.22), assignable to the absorptions endemic to the deprotonated phenol groups.[19] When excited at 350 nm, the solution of Ce–**ZPS** (10 μM) gave an initially weak emission. The addition of the RDX (1 μM) caused a *ca.* 8-fold luminescent enhancement after a 5 min irradiation with 310 nm light at 298 K (Fig. 2). The addition of other explosives such as pentaerythritol tetranitrate (PETN), 2,4,6-trinitrotoluene (TNT), 2,6-dinitrotoluene (DNT), 2-nitro-toluene (NT), 1,4-dinitrobenzene (DNB), nitrobenzene (NB), 4-nitrophenol (NP) and picric acid (PA) did not cause any significant luminescence variation. The competition experiments of Ce–**ZPS** (10 μM) in the same solution revealed that the fluorescence responses of RDX (1 μM) were unaffected in the presence of other explosives (up to 10 μM), demonstrating the high selectivity of the Ce–**ZPS** toward RDX over other nitramine explosives. Under optimized conditions, with the concentration of Ce–**ZPS** fixed at 5 μM, the fluorescence intensity of the Ce–**ZPS** solution is nearly proportional to the RDX concentration. And the addition of 10 ppb caused about 50% luminescent enhancement of the solution. It is postulated that the intensity enhancement contributed to the formation of the NAD^+ analogue, whereas the selectivity and the sensitivity were reasonably attributed to the encapsulation of the RDX within the cavity of the tetrahedron to enforce the proximity between RDX and the reducing site of DHPA, giving a more quick and sensitive response towards RDX. To the best of our knowledge, Ce–**ZPS** represents the first example of the metal–organic polyhedral chemosensors for explosive detection in solution.

As the N_2O chelator and the DHPA reductive triggers were robust enough, our fabrication strategy could be extended to other Werner-type capsules composed of transition metal ions. Ligand H_3**ZPT** was obtained by a similar Schiff based formation reaction using 2-pyridyl aldehyde and malonohydrazide in an ethanol solution. The metal–organic octahedron was constructed using zinc ions with a d^{10} electron configuration and ligand H_3**ZPT** through the same strategy.[20] EA and ^{1}H NMR suggested the formation of a new compound in the solution. ESI-MS spectra of the assembly species exhibited an intense peak at m/z = 1027.51 with the isotopic distribution patterns separated by 0.33 Da. The peak was assigned to $[Zn_6(H\mathbf{ZPT})_3(\mathbf{ZPT})]^{3+}$ species, indicating the successful assembly of a Zn_6L_4 molecular octahedron in solution (Fig. 3). Upon the addition of RDX, ESI-MS spectra exhibited a new peak at m/z = 1101.52 with the isotopic distribution patterns separated by 0.33 Da. The peak is assignable to $[Zn_6(H\mathbf{ZPT})_3(\mathbf{ZPT}) \supset RDX]^{3+}$ species by the comparison of this peak with the simulation results obtained on the basis of natural isotopic abundances. These results also demonstrated the formation of a 1:1 host–guest complex,

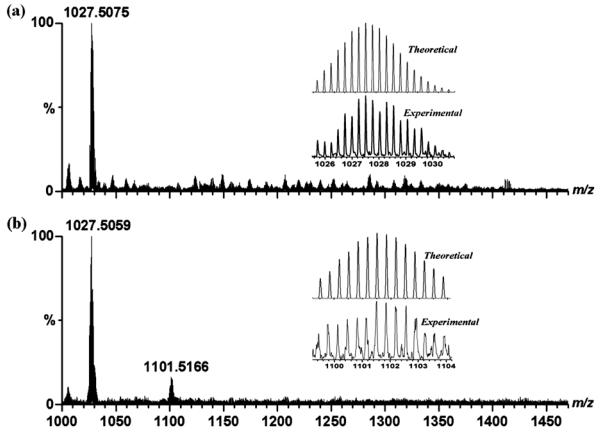

Fig. 3 ESI-MS spectra of (a) Zn–**ZPT** (0.1 mM) and (b) Zn–**ZPT** (0.1 mM) upon addition of 1 equiv. of RDX without illumination in a DMF–CH_3CN solution. Insets display the measured and simulated isotopic patterns at 1027.51 (top picture) and 1101.52 (bottom picture), respectively.

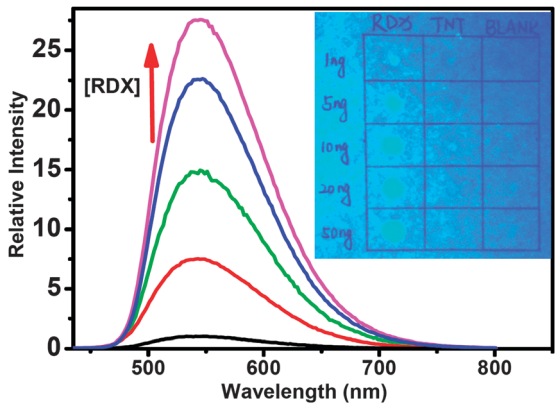

Fig. 4 The time-dependent fluorescence growth of Zn–**ZPT** (10 μM) in a DMF solution upon addition of RDX (1 μM) after irradiation with 310 nm light. Spectra were recorded at time intervals of 1 min. Excited at 415 nm. The inset displays visual fluorescence detection of RDX.

providing the possibility to interact with RDX in the cavity to prompt the formation of luminescent active species efficiently.

Zn–**ZPT** exhibited clear ligand-based charge-transfer bands (at about 300 and 415 nm) in a DMF solution (10 μM). The addition of RDX and irradiation (310 nm) caused a significant decrease in the absorbance intensity at 415 nm and a clear increase at 330 nm. The presence of sharp isosbestic points at 315 and 345 nm indicates that only the reduction and oxidization states of the NADH analogue coexist in equilibrium. When excited at 415 nm, Zn–**ZPT** (10 μM) in DMF exhibited a weak emission band centered at 545 nm. The addition of the RDX (1 μM) caused a *ca.* 27 fold luminescent enhancement after a 5 min irradiation with 310 nm light (Fig. 4). The competition experiments showed that the fluorescence responses of RDX (1 μM) were unaffected in the presence of other explosives (10 μM). The results showed that the two compounds with different metal centres showed similar fluorescence enhancement, which should be due to the formation of a NAD^+ analogue.

Under optimized conditions, with the concentration of Zn–**ZPT** fixed at 5 μM, the fluorescence intensity of the Zn–**ZPT** solution is nearly proportional to the RDX concentration, and the addition of 1 ppb RDX causes about 20% fluorescent enhancement within 5 min. The detection limit of 1 ppb represents the most sensitive chemosensor for RDX in solution. This more sensitive detection compared to the mass spectrometric detection[21,22] suggests the opportunity for its application in the field of rapid detection of trace amounts of explosives.

In order to detect explosive RDX in real world applications, the visual detection study of RDX was performed by preparing substrates spotted with Zn–**ZPT** and explosive RDX solution using DMF–acetonitrile as the solvent. The mixed solutions of Zn–**ZPT** (5 μM) and the desired RDX concentration were spotted onto a filter paper with low background fluorescence using a glass microsyringe. A solvent blank was spotted next to each explosive. After a 1 min irradiation with a 310 nm light, while RDX shows turn-on fluorescence detection as low as 1 ng, other explosives do not show any turn-on fluorescence even for spot loadings as high as 50 ng.

This work was supported by NSFC 21171029 and 21025102 and the Program for Changjiang Scholars and Innovative Research Team in University (IRT1213).

Notes and references

1 J. I. Steinfeld and J. Wormhoudt, *Annu. Rev. Phys. Chem.*, 1998, **49**, 203.
2 K. D. Smith, B. R. McCord, W. A. McCrehan, K. Mount and W. F. Rowe, *J. Forensic Sci.*, 1999, **44**, 789.
3 A. M. Rouhi, *Chem. Eng. News*, 1997, **75**, 14.
4 S. J. Toal and W. C. Trogler, *J. Mater. Chem.*, 2006, **16**, 2871; J.-S. Yang and T. M. Swager, *J. Am. Chem. Soc.*, 1998, **120**, 5321.
5 H. Sohn, M. J. Sailor, D. Magde and W. C. Trogler, *J. Am. Chem. Soc.*, 2003, **125**, 3821; S. J. Toal, D. Magde and W. C. Trogler, *Chem. Commun.*, 2005, 5465.
6 J. Wang, R. K. Bhada, J. Lu and D. MacDonald, *Anal. Chim. Acta*, 1998, **361**, 85; S. Hrapovic, E. Majid, Y. Liu, K. Male and J. H. T. Luong, *Anal. Chem.*, 2006, **78**, 5504.
7 H.-X. Zhang, A.-M. Cao, J.-S. Hu, L.-J. Wan and S.-T. Lee, *Anal. Chem.*, 2006, **78**, 1967; J. Wang, *Electroanalysis*, 2007, **19**, 415.
8 T. L. Andrew and T. M. Swager, *J. Am. Chem. Soc.*, 2007, **129**, 7254.
9 R. Freeman and I. Willner, *Nano Lett.*, 2009, **9**, 322.
10 M. Yoshizawa, J. K. Klosterman and M. Fujita, *Angew. Chem., Int. Ed.*, 2009, **48**, 3418.
11 L. Cronin, *Angew. Chem., Int. Ed.*, 2006, **45**, 3576.
12 A. Lützen, *Angew. Chem., Int. Ed.*, 2005, **44**, 1000.
13 M. D. Pluth, R. G. Bergman and K. N. Raymond, *Acc. Chem. Res.*, 2009, **42**, 1650.
14 J. Hamacek, G. Bernardinelli and Y. Filinchuk, *Eur. J. Inorg. Chem.*, 2008, 3419.
15 D. M. Vriezema, M. C. Aragonès, J. A. A. W. Elemans, J. J. L. M. Cornelissen, A. E. Rowan and R. J. M. Nolte, *Chem. Rev.*, 2005, **105**, 1445; M. Yoshizawa, J. K. Klosterman and M. Fujita, *Angew. Chem., Int. Ed.*, 2009, **48**, 3418.
16 Q. Chen, K. Gao, Y. Duan, Z. Ye, L. Shi, Y. Yang and Y. Zhou, *J. Am. Chem. Soc.*, 2012, **134**, 2442.
17 Crystal data: Ce–**ZBS** $Ce_4C_{170}H_{143}N_{29}O_{30}$: $Ce_4(C_{41}H_{30}N_7O_6)_4{\cdot}C_3H_7NO{\cdot}3CH_3OH{\cdot}2H_2O$, M = 3632.61, tetragonal, space group $P4_2/n$, black block, a = 18.598(3) Å, c = 31.814(6) Å, V = 11004(3) Å^3, Z = 2, D_c = 1.096 g cm^{-3}, μ(Mo-K$_\alpha$) = 0.872 mm^{-1}, T = 180(2) K. 9689 unique reflections [R_{int} = 0.0751]. Final R_1 [with $I > 2\sigma(I)$] = 0.0710, wR_2 (all data) = 0.2566. CCDC number 972499.
18 A. M. Stadler and J. Harrowfield, *Inorg. Chim. Acta*, 2009, **362**, 4298.
19 I. K. Biernacka, A. Bartecki and K. Kurzak, *Polyhedron*, 2003, **22**, 997.
20 C. He, Z. Lin, Z. He, C. Duan, C. Xu, Z. Wang and C. Yan, *Angew. Chem., Int. Ed.*, 2008, **47**, 877.
21 R. Mu, H. Shi, Y. Yuan, A. Karnjanapiboonwong, J. G. Burken and Y. Ma, *Anal. Chem.*, 2012, **84**, 3427.
22 L. Ma, B. Xin and Y. Chen, *Analyst*, 2012, **137**, 1730.